Managing evaporation for more robust microscale assays. Part 1: Volume loss in droplet based assays Supplementary Information.

Erwin Berthier, Jay Warrick, Hongmei Yu and David J. Beebe*

Feb 29, 2008

Contents

APPENDIX I
Mass saturation concentration of water

The water vapor mass concentration C_0 at the interface of the drop is equal to the saturation concentration and can be estimated as a function of the temperature T using the empirical fit for temperature under 40 degrees:

$$C_{sat} = 5.018 + 0.323T + 8.185 \cdot 10^{-3} T^2 + 3.124 \cdot 10^{-4} T^3 \quad (1)$$

Equation (1) states the mass saturation concentration for pure water. For a liquid of different osmolarity, the saturation concentration is given by the Raoult law, where x is the molar fraction of solute:

$$C_{sat}[x] = (1 - x) C_{sat}$$

APPENDIX II
Evaporation of a droplet

In the case of a hemispherical droplet of radius R, the evaporation is proportional to the radius and ΔC_{sat-i}, the water vapor concentration difference between the surface of the drop and the air around it. In the general case of a spherical cap of height H, the evaporation rate is written in function of the height H, which can be expressed in function of the contact angle using Appendix 4:

$$E = \frac{2\pi D}{\rho} \Delta C_{sat-i} H = \lambda H \quad (2)$$

APPENDIX III
Evaporation number

A. Equilibration time

Humidity in an Omnitray has been measured after closing the container to determine the time to achieve equilibration. An Omnitray has been modified to allow the insertion of a humidity probe tip and sealed using BlueTak. One hundred 10μL drops were placed in the Omnitray and the lid was either placed on the container or sealed using BlueTak. Recording of the humidity was effectuated by hand (fig.1).

B. Continuous fluid loss due to temperature gradients.

The importance of fluid loss due to temperature gradients has been characterized by creating controlled temperature gradients using a Pelletier heater/cooler. One hundred 10μL drops were placed in a sealed Omnitray itself placed the heater. A temperature probe was taped inside the Omnitray on the bottom and on the top to measure the effective temperature gradient inside the container. For a 5 degrees temperature difference, total evaporation was achieved in less than 5 hours.

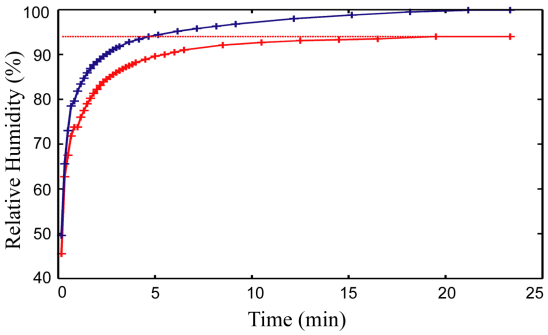

Figure 1: (Color Online) Humidity equilibration in a parafilm-sealed Omnitray (top line) and in a closed Omnitray (bottom line).

C. Evaporation Number

Evaluation of volume changes and the subsequent osmolarity variations can be performed using the evaporation number (3) with contributions from the initial evaporation number to reach saturation (4) and evaporation number for leaks (5) or temperature gradients (6):

$$Ev = Ev_{ini} + Ev_{Leak} + Ev_{Tgrad} \tag{3}$$

$$EV_{ini} = \frac{\sum R_i}{\sum R}\frac{C_{sat}V_a}{\rho V_i} \tag{4}$$

$$Ev_{Leak} = \frac{\sum R_i}{\sum R}\frac{D\Delta C_{i-e}\Delta t}{\rho V_i}\zeta \tag{5}$$

$$Ev_{Tgrad} = \sum R_i \frac{D(C_{sat}(T) - C_{sat}(T - dT))\Delta t}{\rho V_i} \tag{6}$$

D. Liquid with a different osmolarity

If the liquid of interest has a large osmoarity, the saturation concentration of the liquid will be reduced. A difference of osmolarity in the drop n, causes a variation of ΔC_{sat-i} to ΔC_n. This decreases the evaporation rate, which can be written by using the same arguments as for pure water:

For pure water:

$$E = \frac{2\pi D}{\rho}\Delta C_{sat-i}R = \lambda R \tag{7}$$

For different osmolarity:

$$E = \frac{2\pi D}{\rho}\Delta C_n R = \frac{\Delta C_n}{\Delta Csat_i}\lambda R \tag{8}$$

Thus the fraction of unwanted evaporation, χ, (ratio of evaporation on the drops of interest with the total evaporation on all the drops) will be shifted accordingly, with x_i the molar fraction of compounds participating in changing the osmolarity of the liquid:

$$\chi = \frac{\sum E_i}{\sum E_n} = \frac{\sum \Delta C_i R_i}{\sum \Delta C_n R_n} = \frac{\sum (1 - \frac{x_i}{C_w})R_i}{\sum (1 - \frac{x_n}{C_w})R_n} \tag{9}$$

APPENDIX IV
Trigonometric relationships in a spherical cap

A. Lengths

Following are the different relation ships in spherical caps linking geometrical parameters to each other.

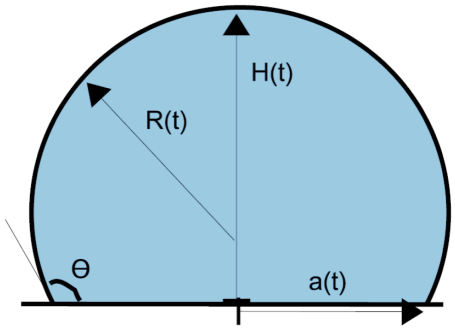

Figure 2: Spherical cap of Radius R and height H.

To express R in function of H and a:

$$R(t) = \frac{H(t)^2 + a^2}{2H(t)}$$

H in function of the contact angle and R:

$$H(t) = (1 - \cos\theta)R(t)$$

Finally a in function of R and the contact angle θ:

$$a(t) = R(t)\sin\theta$$

B. Areas

The surface area of the spherical cap is:

$$S(t) = 2\pi R(t)H(t)$$

C. Volumes

The volume V can be written in function of the wetted radius and the height:

$$V = \frac{\pi}{6}H(t)(3a^2 + H(t)^2)$$

Or in function of the contact angle and the height:

$$V = \frac{\pi(2 - 3\cos\theta + \cos^3\theta)}{3(1 - \cos\theta)^3}H^3 = g(\theta)H^3$$

Or in function of the contact angle and the wetted radius:

$$V = \frac{\pi(2 - 3\cos\theta + \cos^3\theta)}{3}\frac{a^3}{\sin^3\theta} = f(\theta)\frac{a^3}{\sin^3\theta}$$

APPENDIX V
Evaporation from arrays of large number

The approach used here to analyze evaporation is taken from electrostatics where, at steady state, the

potential field, ϕ and concentration field, C, are solutions to the same harmonic differential equations as shown in Eq 10. Thus, an analogy can be made between potential and concentration. The similarity between diffusion and electrostatics has been leveraged in other applications such as analysis of soluble cell signaling via autocrine factors[1,2]. Using the analogy between potential and concentration further, the electric field can be compared to molecular flux per unit area (see Eq 11). Now notice that from Gauss's law in electrostatics, the charge, Q, contained within a bounding surface can be calculated similarly to the total molecular flux, J, entering a surface as shown by Eq 12.

$$\nabla^2\phi = 0 \;\sim\; \nabla^2 C = 0 \tag{10}$$

$$E = \nabla\phi \;\sim\; F = -D\nabla C \tag{11}$$

$$Q = \frac{1}{4\pi}\int_S EdS \;\sim\; J = \int_S FdS \tag{12}$$

We know from electrostatics that the potential of an object can be calculated using the capacitance, ζ, and charge, q, as shown in Eq 13 where ζ has units of [cm] in the cgs system and $\Delta\phi$ is the difference in the potential at the object and at infinity. Using the analogies described thus far and Eq 13, Eq 14 can be derived for the flux to or from an infinitely absorbing or producing body of arbitrary shape suspended in an infinite medium. Thus, to find the diffusive flux, we need only the equivalent electrical capacitance of the shape. For a sphere in cgs units, $\zeta = r$ where r is the radius of the sphere giving $J = 4\pi r D\Delta C$, which matches the solution derived directly from the diffusion equation. The power of this method is not only the ability to use solutions for capacitances of many shapes but also to estimate the capacitances of arrays of shapes, which is crucial to the scaling of microassays.

$$\Delta\phi = \frac{q}{\zeta} \tag{13}$$

$$J = 4\pi D\zeta\,\Delta C \tag{14}$$

Two general geometries will be analyzed. The first geometry is that of a single fluid-air interface and the second is an array of fluid-air interfaces. The influence of the shape of an individual fluid-air interface can be substituted in afterward using equations for the capacitances. Two shapes of particular interest are of a sphere and a disk, given by Eq 15 and 16.

$$\zeta_{sphere} = r \tag{15}$$

$$\zeta_{disk} = \frac{2r}{\pi} \tag{16}$$

In order to estimate the flux to or from the array, the capacitance of the array is estimated following the method outlined by Berg and Purcell[1]. In brief, if the size of the individual conductors is small compared to the spacing of the conductors, then the electrical potential near an individual conductor can be estimated as the potential due to the nearest interface, q/ζ_{int}, plus the potential due to the rest of the array, $(N-1)q/\zeta_{array}$. Thus, the potential has two main contributions, the nearby interface and the rest of the interfaces, which are far enough away to appear as a large uniform interface with geometry matching the array. Thus, the total capacitance of the array can be calculated as the ratio of total charge to total potential, shown in Eq 17. ζ_{int} depends on the shape and size of the individual interfaces, whereas ζ_{array} depends on the overall shape and size of the array. In our case ζ_{int} will either be a hemisphere, $r/2$, or a disk, r/π, where r is the radius of the interface. ζ_{array} will be given as a/π where a is the radius of the array assuming a disk-like pattern. Another important assumption of this method is that the interfaces are quite uniformly distributed. Interfaces that are too close together would behave more like an individual interface of a different shape and thus reduce N and change ζ_{int}.

$$\frac{Nq}{\frac{q}{\zeta_{int}} + \frac{(N-1)q}{\zeta_{array}}} \tag{17}$$

Two solutions will be of particular focus. Eq 18 gives the flux to a disk shaped array of disk shaped interfaces while Eq 19 gives the flux to a disk shaped array of hemispherical interfaces. The capacitance for a disk shaped air-fluid interface is only r/π, which is half that stated in Eq 16 because there is flux to only one side of a disk instead of to both sides. Similarly the capacitance of a hemisphere is half that of a sphere.

$$J_{disk} = 4aD\Delta C\left(\frac{1}{1+\frac{1}{N}(\frac{a}{r}-1)}\right) \tag{18}$$

$$J_{hemi} = 4aD\Delta C\left(\frac{1}{1+\frac{1}{N}(\frac{2a}{\pi r}-1)}\right) \tag{19}$$

If we make the assumption $N \approx (N-1)$ to simplify the equations we get.

$$J_{disk} = 4aD\Delta C\left(\frac{1}{1+\frac{a}{Nr}}\right) \tag{20}$$

$$J_{hemi} = 4aD\Delta C\left(1+\frac{1}{\frac{2a}{\pi Nr}}\right) \tag{21}$$

There is immediate insight into the behavior of the system using Eq 20 and 21. The portion of the equations in front of the parentheses is N times the maximum flux of an individual interface. Most importantly, instead of being linear with N, the total flux increases with N but level off to a maximum value. The equation can be rearranged to see that the maximum of either equation is the flux of a one sided disk of radius a, $J_{max} = 4aD\Delta C$. J_{max} is achieved when the interfaces sufficiently cover the array to act as a single uniform surface yet the ratio of areas, Nr^2/a^2, is still $\ll 1$. Remarkably, J_{max} can be approached for very small values of Nr^2/a^2 if r is sufficiently smaller than a.

A limitation of Eq 20 and 21 is that they neglect convective effects. However, convective effects can often be modeled using a constant multiplier that is a function of the fluid velocity. Therefore, although the equations are limited to zero convection when predicting fluxes, the behavior of flux with respect to the number of surfaces remains relatively unchanged.

The effects of convection on flux have also been treated before by Purcell[3] and used as justification by Lauffenburger[2] in cell signaling analysis. The dimensionless quantity $u = \Omega a^2/D$ was experimentally verified as a measure of the fractional increase in flux due to convection around a sphere where Ω is the shear. The experimental also suggested that flux increases less than 10% for values of u less than one.

With Eq 20 and 21, evaporation in microdevices can be evaluated with insight into the effect of array spacing, interface size, interface shape, temperature, humidity, and osmolarity. The results will also allow us to relate evaporation measured for an array of number N and estimate the evaporation for an array of increased number M.

References

1. D. Lauffenburger and C. Cozens, *Biotechnology and Engineering*, 1989, **33**, 1365-1378.

2. H. C. Berg and E. M. Purcell, *Biophysical Journal*, 1977, **20**, 193-219.

3. E. M. Purcell, *Journal of Fluid Mechanics*, 1978, **84**, 551-559.